Large linear magnetoelectric effect induced by an external magnetic field in the collinear antiferromagnet $DyCrO_4$

M. V. Eremin [*]
Institute of Physics, Kazan Federal University, 420008 Kazan, Russia

(Received 22 March 2020; revised 18 May 2020; accepted 31 August 2020; published 21 September 2020)

A microscopic theory of the interaction of Cr spins with electric and magnetic fields in $DyCrO_4$ is described. The derived effective energy operator allows calculating the electric polarization vector using information about the magnetic structure. The calculated linear electric polarization in electric and magnetic fields at $H < 3$ T is consistent with the available experimental data. The electric field is induced by an odd crystalline field on chromium ions and the charge transfer process from the nearest oxygen ions. The enhancement of the magnetic field is associated with magnetic susceptibility, mainly due to dysprosium ions.

DOI: 10.1103/PhysRevB.102.104107

I. INTRODUCTION

Transition-metal compounds with magnetoelectric coupling attract significant interest in modern science as they can find applications in new technical devices. They are also of considerable importance for fundamental science [1–4]. Experimental searches for substances with electromagnetic properties are continuing. Relevant recent reviews are given in Refs. [5,6]. The development of a microscopic theory of magnetoelectric coupling is also highly desirable. Recently, an anomalously large increase in electrical polarization when an external magnetic field is applied was discovered (with no clear origin) in $DyCrO_4$ [7]. An overview of the currently under discussion mechanisms of magnetoelectric coupling is given in Ref. [6]. Magnetic moments of both Dy^{3+} and Cr^{5+} ions at $T < 20$ K are ordered antiferromagnetically [8,9] and lie in the *ab* plane of the crystal [10,11]. Strict antiparallel ordering of spins means that the known mechanisms of coupling of exchange-coupled spins with an electric field containing a vector product of spins (such as the inverse Dzyaloshinskii-Moriya mechanism and others [5,6]) are not related to the origin of the linear magnetoelectric effect in $DyCrO_4$.

As for other possible mechanisms which do not include the vector product of spins, such as Arima's mechanism [12], the influence of magnetic field arises from changing the spin's direction. However, this effect is relatively weak. So according to Ref. [13], the growth of electric polarization in $(Cu,Ni)B_2O_4$ is about 1.2 $\mu C/m^2$ when the magnetic field is increased by 3 T.

The observed linear magnetoelectric effect in $DyCrO_4$ is anomalously large [7]. When an external field of 1 T is applied, the electric polarization reaches $P \approx 45$ $\mu C/m^2$. When the magnetic field increases to 2 T, it becomes equal to 90 $\mu C/m^2$. Below we present a quantum theory to explain this anomalously large linear magnetoelectric effect and demonstrate how it can be explained by the joint action of spin-orbit interaction and electromagnetic fields induced inside the crystal by external **E** and **H** fields.

II. ENERGY LEVELS OF THE LOW-LYING Cr^{5+} STATE

$Cr^{5+}(3d)$ ions are placed in the tetrahedral sites of oxygen ions (see Fig. 1). In the unit cell, there are two types of fragments, $Cr(1)O_4$ and $Cr(2)O_4$, which are rotated with respect to each other by 90° around the *c* axis. The operator of the crystal electric field (CEF) is written as

$$H_{cf} = \sum_{k,q} B_q^{(k)} C_q^{(k)}, \tag{1}$$

where

$$C_q^{(k)} = \sqrt{\frac{4\pi}{2k+1}} \sum_i Y_{k,q}(\vartheta_i, \varphi_i) \tag{2}$$

are CEF operators acting on $3d$ electrons. The coefficients $B_q^{(k)}$ can be calculated in the superposition model [14,15] as follows:

$$B_q^{(k)} = \sum_j a^{(k)}(R_j)(-1)^q C_{-q}^{(k)}(\Theta_j, \Phi_j). \tag{3}$$

The index j runs over the ions that surround the CrA1 position of the crystal lattice. $a^{(k)}(R_j)$ are the so-called intrinsic CEF parameters. Their three key contributions are

$$a^{(k)}(R_j) = a^{(k)}(p.c.) + a^{(k)}(kl) + a^{(k)}(ex). \tag{4}$$

The first one is due to the point charges of the lattice ions and is given by the expression [16]

$$a^{(k)}(p.c.) = -\frac{Z_j e^2}{R_j^{k+1}} \langle r^k \rangle, \tag{5}$$

where R_j is the distance to ion j, Z_j is the electric charge of ion j in units of $|e|$, and $\langle r^k \rangle$ are averages calculated with radial functions of $3d$ electrons.

The electrostatic field from the spatial distribution of the electron density of the $2s$ and $2p$ electrons of the ligand ions

---

[*] meremin@kpfu.ru

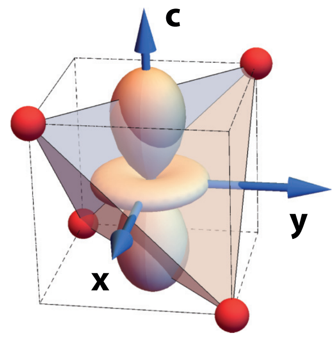

FIG. 1. A fragment of the Cr(1)O$_4$ structure. Cr is in the position (1/2, 1/4, 3/8). The local coordinate system **xy** is rotated around the crystallographic **c** axis by an angle $\varphi = -8.94^\circ$. Oxygen ions are located at the vertices of a tetrahedron, which is slightly shortened along the c axis. Here $\cos(\vartheta) = \pm 0.5073$; that is, it is larger than in the case of a regular tetrahedron, where it is ± 0.5774. The distances between the chromium and oxygen ions are the same and at $T = 1.2$ K are equal to 1.702 Å.

(oxygen) was calculated using the following equations [17]:

$$a^{(2)}(kl) = \langle 3d0|V|3d0\rangle + \langle 3d1|V|3d1\rangle - 2\langle 3d2|V|3d2\rangle,$$
$$a^{(4)}(kl) = (9/5)\langle 3d0|V|3d0\rangle - (12/5)\langle 3d1|V|3d1\rangle + (3/5)\langle 3d2|V|3d2\rangle. \quad (6)$$

Matrix elements are calculated for a separate Fe^{2+}-O$^{2}(j)$ pair in local coordinate systems with a common z axis directed along the pair axis. The expression for the potential energy of a $3d$ electron V is written as [17]

$$V(r) = \frac{e^2}{r}\sum p_i \exp(-\gamma_i r^2). \quad (7)$$

Here, $r = 0$ corresponds to the position of the jth nucleus of the oxygen ion. The importance of this contribution, which substantially suppresses the CEF of point charges, was first pointed out by Kleiner [18]. In this regard, we denote it as $a^{(k)}(kl)$. The values of p_i and γ_i were determined in Ref. [17].

The exchange and covalence contributions related to the overlap of the wave functions of Fe ions with those of the nearest oxygen ions were calculated as [19]

$$a^{(2)}(ex) = \frac{G_2 e^2}{R_j}\left(S_{3d\sigma}^2 + S_{3ds}^2 + S_{3d\pi}^2\right),$$
$$a^{(4)}(ex) = \frac{9G_4 e^2}{5R_j}\left(S_{3d\sigma}^2 + S_{3ds}^2 - \frac{4}{3}S_{3d\pi}^2\right), \quad (8)$$

where G_2 and G_4 are the fitting parameters of the exchange charge model [19]. They are determined by comparing theoretical and experimental data. The quantities $S_{3d\sigma}$, S_{3ds}, and $S_{3d\pi}$ are the overlap integrals for a separate Fe^{2+}-O$^{2-}(j)$ pair in local coordinate systems with a common z axis directed along the pair axis. We evaluated these integrals using the Hartree-Fock wave functions of free ions [20,21], previously expanded in Gaussian orbitals. The calculated values of $a^{(k)}$ for the nearest-neighbor oxygen ions ($R = 1.702$ Å and $G_2 = G_4 = 9$) are given in Table I.

TABLE I. Calculated values of $a^{(k)}$ (in cm^{-1}).

	$a^{(k)}(p.c.)$	$a^{(k)}(ex)$	$a^{(k)}(kl)$	Sum
$a^{(2)}$	14192	7239	−15042	6389
$a^{(4)}$	2783	6682	−4836	4629

Summing (3) over lattice ions, we have (in cm^{-1})

$$B_0^{(2)} = -2911, \quad B_0^{(4)} = -5562, \quad B_4^{(4)} = -5340. \quad (9)$$

It should be noted that the contribution to the parameter $B_0^{(2)}$ associated with lattice ions at a distance of $R > 1.702$ Å is equal to 844 cm^{-1}. The corresponding contributions to $B_0^{(4)}$ and $B_4^{(4)}$ are relatively small.

The energy levels of a $3d$ electron are (in cm^{-1})

$$E_\vartheta = \frac{2}{7}\left(B_0^{(2)} + B_0^{(4)}\right) = -2420,$$
$$E_\eta = E_\xi = \frac{1}{7}B_0^{(2)} - \frac{4}{21}B_0^{(4)} = 1438,$$
$$E_\zeta = -\frac{2}{7}B_0^{(2)} + \frac{1}{21}B_0^{(4)} + \frac{5}{3}\sqrt{\frac{2}{35}}\left|B_4^{(4)}\right| = 2695,$$
$$E_\varepsilon = -\frac{2}{7}B_0^{(2)} + \frac{1}{21}B_0^{(4)} - \frac{5}{3}\sqrt{\frac{2}{35}}\left|B_4^{(4)}\right| = -1561. \quad (10)$$

Here, $|\vartheta\rangle = |3z^2 - r^2\rangle$, $|\varepsilon\rangle = |x^2 - y^2\rangle$, $|\eta\rangle = |xz\rangle$, $|\xi\rangle = |yz\rangle$, and $|\zeta\rangle = |xy\rangle$ are the orbital states of the $3d$ electron. Note that the case of an undistorted tetrahedral crystal field can be considered if $B_0^{(2)} = 0$ and $B_{\pm 4}^{(4)} = \pm\sqrt{\frac{5}{14}}B_0^{(4)}$ in (10). The energy level scheme of the Cr^{5+} ion in DyCrO$_4$ has not yet been experimentally studied. According to the optical conductivity spectra of FeCr$_2$O$_4$, the energy interval between the ^5T and ^5E Fe^{2+} states in the tetrahedral position is ≈3300 cm^{-1} [22].

Neutron diffraction studies [10,11] revealed that at $T = 1.2$ K the magnetic moments of chromium in DyCrO$_4$ lie in the ab plane, and their values are relatively small ($\mu_{x,y} = 0.99\mu_B \pm 0.12\mu_B$). We calculated the following components of the g tensor for the ground state:

$$g_{x,y} = 2 - \frac{6\lambda}{E_{\eta,\xi} - E_\vartheta} \cong 1.71, \quad g_z = 2. \quad (11)$$

Qualitatively, this result ($g_{x,y} < 2$) confirms our conclusion that the ground state of Cr^{5+} is indeed $|\vartheta\rangle = |3z^2 - r^2\rangle$. However, perhaps, the calculated value of $E_{\eta,\xi} - E_\vartheta$ is overestimated. In (11), λ is the parameter of the spin-orbit coupling. Its value, determined from the energy level scheme of the free Cr$^{5+}(3d)$ ion [23], is 188 cm^{-1}.

III. INTERACTION ENERGY OF A 3*d* ELECTRON WITH ELECTRIC AND MAGNETIC FIELDS

In the superposition model, the energy of the MeO$_4$ fragment is determined by the sum of energies of separate Me-O pairs. The basic electronic configuration of the metal ion is Cr$^{5+}(3d)$, and that of the oxygen ion is O$^{2-}(1s^2 2s^2 2p^6)$. The lowest excited configurations of opposite parity in the chromium-oxygen pair are Cr$^{5+}(4p)$ O$^{2-}(1s^2 2s^2 2p^6)$, and the so-called charge transfer configurations are Cr$^{4+}(3d^2)$

$O^{1-}(1s^2 2s^2 2p^5)$ and $Cr^{4+}(3d^2)$ $O^{1-}(1s^2 2s^1 2p^6)$. The processes of electron transfer from ligands to the unfilled shell of a metal ion play an important role in the theory of the electronic structure of complexes and paramagnetic centers. Usually, they are taken into account by the method of linear combinations of atomic orbits [16]. However, in our case, the method of superposition of configurations is preferable since it allows one to consider structural fragments with arbitrary symmetry and to use the operator technique of atomic spectroscopy [24].

The development of the theory of interaction between electronic configurations of opposite parity nl^N and $nl^{N-1}n'l'$ was stimulated by the problem of explaining parity-forbidden electric dipole transitions between multiplets of the nl^N configuration in crystals without an inversion center. A calculation method based on the technique of irreducible tensor operators was first developed in Refs. [25,26].

The effective operator of electric dipole transitions was obtained in the second order of the perturbation theory by combining the operator of an odd crystal field with the operator of the energy of interaction of electrons with an electric field. It is useful to write it as follows:

$$H_E = \sum_{p,t,k} \{E^{(1)} U^{(k)}\}_t^{(p)} D_t^{(1k)p}. \tag{12}$$

Here, the curly brackets denote the Kronecker product of the spherical components of the electric field

$$E_0^{(1)} = E_z, \quad E_{\pm 1}^{(1)} = \mp (E_x \pm i E_y)/\sqrt{2}, \tag{13}$$

and $U_q^{(k)} = \sum_i u_q^{(k)}(i)$ are the components of the unit irreducible tensor operator, acting on $3d$ electron states. Single-electron matrix elements of operators $u_q^{(k)}$ are calculated through 3-j symbols,

$$\langle lm | u_q^{(k)} | lm' \rangle = (-1)^{l-m} \begin{pmatrix} l & k & l \\ -m & q & m' \end{pmatrix}. \tag{14}$$

The quantities $D_t^{(1k)p}$ are evaluated, in the case of a spherical electron density distribution on the ligands, by the expression

$$D_t^{(1k)p} = \sum_j d^{(1k)p}(R_j)(-1)^t C_{-t}^{(p)}(\vartheta_j \varphi_j), \tag{15}$$

where $C_{-t}^{(p)}(\vartheta_j, \varphi_j)$ are the components of the spherical tensor that determines the orientation of the selected metal-ligand pair (j is the ligand number) with respect to the crystallographic coordinate system. The contribution to $d_j^{(1k)p}$ associated with mixing of nl^N and $nl^{N-1}n'l'$ configurations are evaluated as follows:

$$\begin{aligned} d_j^{(1k)p}(1) = {} & \frac{2|e|\langle r \rangle_{ll'}}{|\Delta_{ll'}|\sqrt{2p+1}} (2k+1)(l\|c^{(1)}\|l') \\ & \times (l'\|c^{(k)}\|l) \begin{Bmatrix} 1 & k & p \\ l & l' & l \end{Bmatrix} \left(\frac{\epsilon' + 2}{3} \right) a^{(k)}(R_j), \end{aligned} \tag{16}$$

where ϵ' is the real part of the dielectric permittivity. The Lorentz correction factor $(\epsilon' + 2)/3$ was originally omitted in the Judd-Offelt expressions. Later, it was included in the theory and plays an important role in our case. Thus, according to the experimental data [7], ϵ' for $DyCrO_4$ is approximately equal to 13, and therefore, the Lorentz factor enhances the action of the electric field by about 5 times.

With expression (16) derived, the operator of an odd crystal field (k is an odd number) is written similarly to (1), i.e.,

$$H_{cr} = \sum_{k,q} B_q^{(k)} C_q^{(k)}, \tag{17}$$

where $C_q^{(k)}$ are spherical tensor operators whose single-electron matrix elements are calculated by the Wigner-Eckart theorem:

$$\begin{aligned} \langle lm | c_q^{(k)} | l'm' \rangle = {} & (-1)^{l-m} \begin{pmatrix} l & k & l' \\ -m & q & m' \end{pmatrix} \\ & \times (l\|c^{(k)}\|l'). \end{aligned} \tag{18}$$

In our case, $l = 2$ and $l' = 1$. From the selection rules of the reduced matrix element $(l||c^{(k)}||l')$ it follows that k can be equal to 1 or 3. Operator (12) is Hermitian at odd values of p. The 6-j symbol limits the possible values of p: p can be equal to 1, 3, or 5.

In the case of spherically symmetrical ligands, the parameters of the odd crystal field are determined by an equation similar to (3). The structure of the CrO_4 fragment is shown in Fig. 1. Group symmetry at the chromium position is the S_4 point symmetry. Invariant combinations of spherical components can be constructed only for $k = 3$. In this case, the lattice sums converge rapidly, and only the contribution of four nearest oxygen ions can be taken in to account to estimate them. In the local coordinate system, as in Fig. 1, the structure factor is equal to

$$\sum_j C_{\pm 2}^{(3)}(\vartheta_j, \varphi_j) = \mp 2.1069 i. \tag{19}$$

To numerically evaluate $a^{(3)}$ and $a^{(5)}$, we used the following expression:

$$\begin{aligned} & a^{(k)}(R_j)_{ll'} \\ & = -\frac{Z_j e^2}{R_j^{k+1}} \langle r^k \rangle_{ll'} + \frac{(2k+1)}{(l||c^{(k)}||l')} \sum (-1)^{l-m} \\ & \quad \times \begin{pmatrix} l & k & l' \\ -m & 0 & m \end{pmatrix} \left\{ \begin{matrix} \frac{G_j e^2}{R_j} \langle nlm | n_j l_j m \rangle \langle n_j l_j m | n'l'm \rangle \\ + \langle nlm | V_j(r_b) | n'l'm \rangle \end{matrix} \right\}. \end{aligned} \tag{20}$$

Here, the first term takes into account the field of point charges of the lattice ions. The second term approximates the effect of the overlapping of the electron shells of metal ions with the nearest ligands (oxygen). $\langle nlm | n_j l_j m \rangle$ are the overlap integrals of the nl states of electrons with wave functions $2s$ and $2p$ of oxygen electrons. G_j is a parameter of the exchange charge model. $V_j(r)$ is the energy of interaction of an nl electron with the electrostatic field of spatially distributed $2s$ and $2p$ electron shells of oxygen [as in (7)].

The results of our calculation of the overlap integrals for the Hartree-Fock wave functions $Cr^{5+}(3d)$ and $O^{2-}(2s, 2p)$ (taken from [27,20], respectively) at $R_j = 1.702$ Å are equal to

$$\begin{aligned} & \langle 3d0 | 2p0 \rangle = -0.0704, \quad \langle 3d1 | 2p1 \rangle = 0.0496, \\ & \langle 3d0 | 2s0 \rangle = -0.0661. \end{aligned} \tag{21}$$

Since the radial Hartree-Fock wave functions for the excited state of $Cr^{5+}(4p)$ have not yet been obtained, we used the wave functions of the excited configuration of the $Fe^{3+}(3d^4 4p)$ ion from [27]. The overlap integrals required for our numerical estimations are equal to

$$\langle 4p0|2p0\rangle = -0.1745, \quad \langle 4p1|2p1\rangle = 0.3070, \\ \langle 4p0|2s0\rangle = -0.4363. \tag{22}$$

The calculation by formula (8) with $G = 9$ and $R_j = 1.702$ Å yields (in cm^{-1})

$$a_{dp}^{(3)} = 9350 + 26\,120 - 11\,758 = 23\,712. \tag{23}$$

Taking $\langle r\rangle_{dp} = 0.55$ a.u. calculated in Ref. [28] using the Hartree-Fock radial functions of $3d$ and $4p$ electrons and the values of the energy interval between the main $3d^6$ and excited configuration $3d^5 4p$ of the Fe^{3+} ion from Ref. [27], we obtained in D unit (1 debye = $|e|$Å)

$$d^{(12)3}(1) = 0.130, \quad d^{(14)3}(1) = 1.058. \tag{24}$$

We now proceed to assess the role of covalence and nonorthogonality of the wave functions of the $3d$ electron and the wave functions of oxygen. The effective Hamiltonian of interaction with an electric field, which takes into account the nonorthogonality of the wave functions and the mixture of excited configurations with charge transfer, i.e., $3d^{N+1}L^{-1}$ to the ground $3d^N L$ configuration, in its tensor structure coincides with the operator (11). In this case, the contribution to the quantities $d_j^{(1k)p}$ appearing in (1) is determined by the following equations:

$$d^{(1k)p}(R_j) = \frac{\epsilon' + 2}{3}\sum_q (-1)^{1-k+q}\sqrt{(2p+1)} \\ \times \begin{pmatrix} 1 & k & p \\ -q & q & 0 \end{pmatrix} d_q^{(k)}(R_j), \tag{25}$$

$$d_q^{(k)}(R_j) = |e|\sum (-1)^{l-m}(2k+1) \\ \times \begin{pmatrix} l & k & l \\ -m & q & m' \end{pmatrix} \langle nlm|r_j c_q^{(1)}|nlm'\rangle, \tag{26}$$

$$\langle nl\mathrm{m}|r_a C_q^{(1)}|nlm'\rangle = \lambda_{m\kappa}\langle\kappa|rC_q^{(1)}|\rho\rangle\lambda_{\rho n'} \\ - \langle nl\mathrm{m}|rC_q^{(1)}|\rho\rangle\lambda_{\rho m'} \\ - \lambda_{m\kappa}\langle\kappa|rC_q^{(1)}|nlm'\rangle, \tag{27}$$

$$\lambda_{\rho m'} = \gamma_{\rho m'} + S_{\rho m'}. \tag{28}$$

For brevity of notation, in (27) and (28) we used $\gamma_{\rho m'}$ for covalence parameters and $S_{\rho m'}$ for the overlap integrals of metal ligands per one metal-ligand pair. The sets of quantum numbers corresponding to the ligand electrons are denoted κ and ρ. One the right-hand side of (27), we assume summation over the quantum numbers κ and ρ. Two-center matrix elements are specified in local coordinate systems with z axes directed along the axis of a metal-ligand pair.

Equations (11) and (25)–(27) are derived by mixing electronic configurations with a nonorthogonal basis of single-electron wave functions. The main stages of calculation are as follows. At the beginning of the perturbation theory with a nonorthogonal basis of many-electron functions, for separately selected pairs of metal ligands, an effective operator was constructed that operates in the states of the basic electronic states of configuration $3d^N L$. Then, an equivalent new effective operator is constructed in the basis of the product of the wave functions of the metal ion and the surrounding metal ligands. In the final stage, all pairs of metal ligands were summed up (approximation of independent bonds). It was assumed that each of the pairs has axial symmetry with respect to the local z axis directed along the axis of the metal-ligand connection line.

When numerically evaluating $d^{(1k)p}$ from (2) using Eqs. (25)–(28), we take the covalence parameters defined for Ni-O and Cr-O pairs in oxides by magnetic resonance methods [29–31]: $\gamma_\sigma \simeq -0.230$, $\gamma_s \simeq -0.027$, $\gamma_\pi \simeq 0.216$. The calculation of two-center matrix elements was carried out using the Hartree-Fock wave functions of Fe^{2+} [21] and O^{2-} [20] ions, which were decomposed into Gaussian-type orbitals. As a result, the following values were obtained (in debyes):

$$d^{(12)3}(2) = -0.983, \quad d^{(14)3}(2) = 0.273, \\ d^{(14)5} = -0.263. \tag{29}$$

It is interesting to note that, in contrast to (20), in (25) there is a contribution with $p = 5$. The corresponding structure factor is

$$\sum_j C_{\pm 2}^{(5)}(\vartheta_j, \varphi_j) = \mp 0.1109i. \tag{30}$$

The total value of $d^{(12)3}$ included in expression (11) is determined by the sum of two contributions:

$$d_j^{(1k)p} = d_j^{(1k)p}(1) + d_j^{(1k)p}(2). \tag{31}$$

Comparing (25) and (20), we note that contributions to $d^{(12)3}$ are associated with the odd crystal field (1), as well as with the overlap and charge transfer (covalence) (2) of opposite signs, with the latter factor being dominant.

As a result, by substituting (24), (33), and structure factors (19) and (30) into expression (15), we obtained (in debyes)

$$D_{\pm 2}^{(12)3} = \pm 1.797i, \quad D_{\pm 2}^{(14)3} = \mp 2.804i, \\ D_{\pm 2}^{(14)5} = \pm 0.029. \tag{32}$$

It should be noted that if we neglect the distortion of the tetrahedral fragment along the c axis (Fig. 1), all $D_q^{(14)5}$ become equal to zero.

As for the $Cr(2)O_4$ fragments that are rotated by 90° relative to $Cr(1)O_4$ around the c axis of the crystal, their corresponding values of $D_t^{(1k)p}$ are obtained from (32) by changing the sign. This can be easily deduced from expression (15).

At the end of this section, we turn to a discussion of the interaction of $Cr^{5+}(3d)$ with a magnetic field. The operator of interaction is written as follows:

$$H_M = \mu_B(\mathbf{l} + 2\mathbf{s})\mathbf{B}, \tag{33}$$

where the magnetic induction is given by $\mathbf{B} = (1 + 4\pi\chi)\mathbf{H}$. Here, χ is the tensor of magnetic susceptibility per cubic centimeter. The measured values of the magnetic susceptibility in the field-culled regime at $T < 20$ K are about 40 emu/mol [32,33]. Turning to CGSE units, we find that $(1 + 4\pi\chi) \approx 7$;

TABLE II. Two-center matrix elements of $rc_q^{(1)}$ (in a.u.) at $R = 1.702$ Å.

Matrix elements	Values
$\langle 3d0\vert rc_0^{(1)}\vert 2p0\rangle$	−0.1400
$\langle 3d1\vert rc_0^{(1)}\vert 2p1\rangle$	0.0949
$\langle 3d0\vert rc_0^{(1)}\vert 2s0\rangle$	−0.1425
$\langle 3d1\vert rc_0^{(1)}\vert 2s0\rangle$	−0.0513
$\langle 3d2\vert rc_0^{(1)}\vert 2p1\rangle$	0.0610
$\langle 3d1\vert rc_0^{(1)}\vert 2p0\rangle$	−0.0649
$\langle 3d0\vert rc_0^{(1)}\vert 2p-1\rangle$	−0.0050

that is, the effective magnetic field H on the orbital momentum is significantly enhanced. The physical reason for this effect is the large value of the magnetic moment of the Dy^{3+} ion. Studies on neutron scattering [10–12] have shown that the magnetic moment of the dysprosium ions is ≃9 times greater than the magnetic moment of chromium ions.

IV. ORIGIN OF LINEAR MAGNETOELECTRIC COUPLING

Having the energy level scheme (Sec. II) and operators of interaction with electric and magnetic fields (Sec. III), we proceed to the derivation of the magnetoelectric coupling operator for the ground $^2E_\vartheta$ state of chromium. To derive the effective operator H_{eff}, we use the following expression corresponding to the third order of the perturbation theory:

$$\langle\alpha|H_{\text{eff}}|\alpha'\rangle = \sum_{\beta,\tau}\frac{\langle\alpha|H_1|\beta\rangle\langle\beta|H_1|\tau\rangle\langle\tau|H_1|\alpha'\rangle}{(E_\beta - E_\alpha)(E_\tau - E_\alpha)}, \tag{34}$$

where the perturbation operator H_1 is the sum of three operators,

$$H_1 = H_E + H_M + \lambda\mathbf{sl}, \tag{35}$$

and symbols $|\beta\rangle$ and $|\tau\rangle$ denote $|\varepsilon\rangle = |x^2 - y^2\rangle$, $|\eta\rangle = |xz\rangle$, $|\xi\rangle = |yz\rangle$, and $|\zeta\rangle = |xy\rangle$. We assume the presence of spin wave functions $|\sigma = \pm 1/2\rangle$, $|\alpha\rangle = |\vartheta, \sigma\rangle$. Since $E_\eta = E_\xi$, it is convenient to take $|d, +1\rangle$ and $|d, -1\rangle$ instead of the wave functions $|\eta\rangle = |xz\rangle$, $|\xi\rangle = |yz\rangle$ in the calculation process.

The scheme of virtual excitation explaining the mechanism of magnetoelectric coupling is shown in Fig. 2. It is interesting to note that the magnetoelectric coupling arises due to the interaction of the orbital moment of the electron with the magnetic field, while the interaction of the spin with the magnetic field does not play any role in this scheme.

The resulting effective operator in the basis of spin states $|^2E_\vartheta, \pm 1/2\rangle$ is

$$\begin{aligned} H_{\text{eff}} = {} & 4\frac{\lambda\mu_B}{\Delta_\varepsilon\Delta}\text{Re}D_1(S_xB_x - S_yB_y)E_z \\ & - 4\frac{\lambda\mu_B}{\Delta_\zeta\Delta}\text{Im}D_1(S_xB_y + S_yB_x)E_z \\ & + 6\frac{\lambda\mu_B}{\Delta^2}\text{Re}D_2(S_xB_x - S_yB_y)E_z \\ & - 6\frac{\lambda\mu_B}{\Delta^2}\text{Im}D_2(S_xB_y + S_yB_x)E_z. \end{aligned} \tag{36}$$

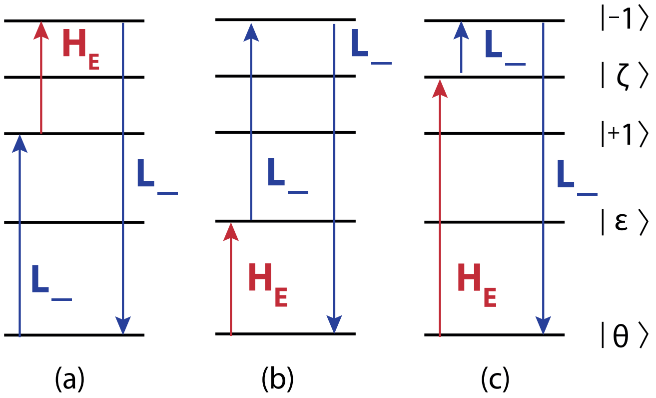

(a) (b) (c)

FIG. 2. Examples of virtual excitation schemes. Operator L_- enters in either the spin-orbit interaction or the interaction of orbital moment with a magnetic field.

Here, Δ_ε, Δ_ζ, and $\Delta = \Delta_\eta = \Delta_\xi$ are the energy intervals between the ground and excited states $|\varepsilon\rangle$, $|\zeta\rangle$, and $|\pm 1\rangle$, respectively. B_x, B_y, and B_z, as in (33), are the components of the effective magnetic field. For brevity, we introduce the following quantities:

$$\begin{aligned} D_1 &= \left\{2\sqrt{\frac{1}{35}}D_2^{(12)3} - \sqrt{\frac{1}{21}}D_2^{(14)3} + \sqrt{\frac{1}{15}}D_2^{(14)5}\right\}, \\ D_2 &= \left\{\sqrt{\frac{1}{35}}D_2^{(12)3} + \frac{2}{3}\sqrt{\frac{1}{21}}D_2^{(14)3} - \frac{2}{3}\sqrt{\frac{1}{15}}D_2^{(14)5}\right\}. \end{aligned} \tag{37}$$

Since $\text{Re}D_1$ and $\text{Im}D_2$ transform similarly to $x^2 - y^2$ and xy under rotation around the z axis, it can be seen from (36) that the contributions from the $DyCr(1)O_4$ and $DyCr(2)O_4$ fragments to the total magnetoelectric energy are equal.

In the coordinate system shown in Fig. 1, we obtained (in D)

$$\text{Im}D_1 = 1.212, \quad \text{Im}D_2 = -0.099. \tag{38}$$

Let's now discuss what follows from Eq. (36). First, there is no electric polarization in zero magnetic field. The next important consequence is that the electric polarization along the z axis increases only when the spins and the magnetic field lie in the ab plane. This is exactly what was observed in Ref. [7] at $H < 3$ T.

Since all quantities included in expression (36) have been determined, we can numerically estimate the linear magnetoelectric effect driven by an external magnetic field. Taking the derivative of the effective energy operator (36) with respect to the electric field component E_z and setting $\langle S_x\rangle = 1/2$, we obtain the electric polarization [in (μC/m^2) T]:

$$\begin{aligned} P_z = {} & \frac{\lambda\mu_B}{\Delta}\left(\frac{2D_1}{\Delta_\zeta} + \frac{3D_2}{\text{Im}\Delta}\right) \\ & \times (1 + 4\pi\chi)NH_y = 42.05H_y, \end{aligned} \tag{39}$$

where N is the number of Cr ions in samples with a volume of 1 m^3. According to experimental data [7], the proportionality coefficient between electric polarization and the magnetic field is about 45 μC/m^2. Thus, the calculated value is in agreement with the experimental data.

Note that an operator form similar to (36) can certainly be obtained from symmetric considerations. This problem was discussed by Ham in 1961 when he investigated the effect of electric fields on the spectra of electron paramagnetic resonance in dilute paramagnets [34,35]. Of course, it was not possible to obtain microscopic expressions for the interaction parameters at that time since the real mechanism of interaction of spins with the electric field was not established. An operator form similar to (36), within the framework of the phenomenological approach for the antiferromagnet Bi_2CuO_4, was proposed in Ref. [36]. In Bi_2CuO_4 there is also no electrical polarization in zero magnetic field. When the magnetic field increases by 1 T, the electrical polarization along the c axis increases (see [36], Fig. 13(b)) by about 0.3 μC/m^2. One of the obvious reasons for such a strong difference from $DyCrO_4$ is that the factor $(1 + 4\pi\chi)$ entering before the magnetic field is relatively small in Bi_2CuO_4. In Bi_2CuO_4 there are no magnetic ions with such a large g factor as the Dy ion has in $DyCrO_4$.

Finally, it should be noted that above we assumed that the magnetic field is sufficiently weak and does not violate collinearity in the direction of antiferromagnetically ordered spins and does not change their orientation. According to [7], at $H > 3$ T, a metamagnetic transition is observed in $DyCrO_4$. In a strong magnetic field, the spin orientations become noncollinear. In this case, operators (36) should be supplemented with terms containing vector products of exchange-coupled spins, similar to those discussed in the review in [19] and in [37,38] for noncollinear ferrimagnets. A discussion of the magnetoelectric properties of $DyCrO_4$ in a strong magnetic field is beyond the scope of this paper.

V. CONCLUDING REMARKS

In this paper, we contributed to the microscopic theory of magnetoelectric coupling of spins with electric and magnetic fields in a collinear antiferromagnet $DyCrO_4$. A simple analytical expression for magnetoelectric coupling energy was derived. The calculated linear electric polarization with respect to the electric and magnetic fields is consistent with the experimental value [16] in order of magnitude. The most important features of the nature of the anomalously large linear magnetoelectric effect are given below.

(1) The electric field at orbital degrees of freedom of chromium ions is enhanced by the odd crystal field from the lattice ions, as well as by the influence of covalent bonds of 3d electrons with the nearest oxygen ions, located at the vertices of the tetrahedron.

(2) The magnetic field acting on the spins of chromium ions is enhanced by the factor $1 + 4\pi\chi \simeq 7$. The dominant contribution to spin susceptibility is associated with dysprosium ions, as they have a large magnetic moment ($9.7\mu_B$).

(3) The action of electric and magnetic fields on orbital degrees of freedom of 3d electrons is transmitted to spins of chromium ions through spin-orbital interaction of 3d electrons.

The described scenario of linear coupling of the electric and magnetic fields with spins is applicable to a wide class of compounds with magnetic ions located in positions without inversion symmetry.

ACKNOWLEDGMENT

I am grateful to K. Vasin for help in preparation of the manuscript and useful remarks. This work was supported by the Russian Science Foundation (Project No. 19-12-00244).

[1] Y. Tokura, Science **312**, 1481 (2006).
[2] S.-W. Cheong and M. Mostovoy, Nat. Mater. **6**, 13 (2007).
[3] D. Khomskii, Physics **2**, 20 (2009).
[4] A. P. Pyatakov and A. K. Zvezdin, Phys. Usp. **55**, 557 (2012).
[5] Y. Tokura, S. Seki, and N. Nagaosa, Rep. Prog. Phys. **77**, 076501 (2014).
[6] D. Shuai, L. Jun-Ming, C. Sang-Wook, and R. Zhifeng, Adv. Phys. **64**, 519 (2015).
[7] S. Xudong, Z. Long, C. Yisheng, W. Yan, L. Zhehong, Y. Yunyu, C. Huibo, C. Dela Cruz, S. Young, J. Changqing, A. Munoz, J. A. Alonso, and Y. Long, NPG Asia Mater. **11**, 50 (2019).
[8] Y. W. Long, L. X. Yang, Y. Yu, F. Y. Li, R. C. Yu, S. Ding, Y. L. Liu, and C. Q. Jin, Phys. Rev. B **74**, 054110 (2006).
[9] Y. W. Long, L. X. Yang, Y. Yu, F. Y. Li, Y. X. Lu, R. C. Yu, Y. L. Liu, and C. Q. Jin, J. Appl. Phys. **103**, 093542 (2008).
[10] A. J. Dos Santos-Garca, E. Climent-Pascual, J. M. Gallardo-Amores, M. G. Rabie, Y. Doi, J. Romero de Paz, B. Beuneu, and R. Saez-Puche, J. Solid State Chem. **194**, 119 (2012).
[11] A. J. Dos Santos-Garcia, E. Climent-Pascual, M. G. Rabie, J. Romero de Paz, J. M. Gallardo Amores, D. Khalyavin, and R. Saez-Puche, J. Phys.: Conf. Ser. **549**, 012021 (2014).
[12] T. Arima, J. Phys. Soc. Jpn. **76**, 073702 (2007).
[13] N. D. Khanh, N. Abe, K. Kubo, M. Akaki, M. Tokunaga, T. Sasaki, and T. Arima, Phys. Rev. B **87**, 184416 (2013).
[14] D. J. Newman, Adv. Phys. **20**, 197 (1971).
[15] M. V. Eremin and A. A. Kornienko, Phys. Status Solidi B **79**, 775 (1977).
[16] A. Abragam and B. Bleaney, *Electron Paramagnetic Resonance of Transition Ions* (Oxford University Press, Oxford, 1970).
[17] V. V. Iglamov and M. V. Eremin, Phys. Solid State **49**, 229 (2007).
[18] W. H. Kleiner, J. Chem. Phys. **20**, 1784 (1952).
[19] B. Z. Malkin, in *Spectroscopy of Solids Containing Rare Earth Ions*, edited by A. A. Kaplyanskii and R. M. Macfarlane, Modern Problems in Condensed Matter Sciences Vol. 21 (Elsevier, Amsterdam, 1987), Chap. 2, pp. 13–50.
[20] E. Clementi and A. D. McLean, Phys. Rev. **133**, A419 (1964).
[21] E. Clementi and C. Roetti, At. Data Nucl. Data Tables **14**, 177 (1974).
[22] K. Ohguchi, Y. Okimoto, T. Ogasawara, Sh. Miyasaka, and Y. Tokura, J. Phys. Soc. Jpn. **77**, 034713 (2008).
[23] J. Sugar and C. Corliss, J. Phys. Chem. Ref. Data **14**(Suppl. 2), 1 (1985).
[24] B. R. Judd, *Operator Techniques in Atomic Spectroscopy* (Princeton University Press, Princeton, 1998), p. 256.

[25] B. R. Judd, Phys. Rev. **127**, 750 (1962).

[26] G. S. Ofelt, J. Chem. Phys. **37**, 511 (1962).

[27] M. Synek, A. E. Rainis, and E. A. Peterson, J. Chem. Phys. **46**, 2039 (1967).

[28] A. A. Kornienko and M. V. Eremin, Fiz. Tverd. Tela (Leningrad) **19**, 52 (1977) [Sov. Phys. Solid State **19**, 29 (1977)].

[29] A. Schoenberg, J. T. Suss, S. Szapiro, and Z. Luz, Solid State Commun. **14**, 811 (1974).

[30] P. Freund, J. Phys. C **7**, L33 (1974).

[31] P. Freund, J. Phys. C **16**, 5039 (1983).

[32] Y. Long, Q. Liu, Y. Lv, R. Yu, and C. Jin, Phys. Rev. B **83**, 024416 (2011).

[33] A. Midya, N. Khan, D. Bhoi, and P. Mandal, Appl. Phys. Lett. **103**, 092402 (2013).

[34] F. S. Ham, Phys. Rev. Lett. **7**, 242 (1961).

[35] G. W. Ludwig and F. S. Ham, Phys. Rev. Lett. **8**, 210 (1962).

[36] L. Zhao, H. Guo, W. Schmidt, K. Nemkovski, M. Mostovoy, and A. C. Komarek, Phys. Rev. B **96**, 054424 (2017).

[37] M. V. Eremin, Phys. Rev. B **100**, 140404(R) (2019).

[38] M. V. Eremin, J. Exp. Theor. Phys. **129**, 990 (2019).